Innovative Approach for Brain Tumor Image Classification with Novel Optimized Feedforward Networks

Raafat Munshi
Faculty of Applied Medical Sciences, King Abdulaziz University, Saudi Arabia
rmonshi@kau.edu.sa

Abstract: *Timely diagnosis and effective treatment planning rely on the accurate classification of brain tumor images. This study proposes a novel approach called Adaptive Moth Flame Optimized Feedforward Neural Network (AMFO-FNN) using Magnetic Resonance Imagin (MRI) for brain tumor classification. The method integrates Gaussian filtering for noise reduction and Gray-Level Co-occurrence Matrix (GLCM) for texture-based feature extraction. Classification is performed using a Feedforward Neural Network (FNN), whose parameters are optimized using an enhanced moth flame optimization algorithm. The model was evaluated on the publicly available Br35H dataset comprising 7,023 MRI images across four categories: meningioma, pituitary tumor, glioma, and no tumor. Applied preprocessing and data augmentation techniques to enhance generalization. Experimental results, validated through five-fold cross-validation, demonstrate the superior performance of AMFO-FNN, achieving 99.14% accuracy, 98.95% precision, 99.21% recall, and 99.08% F1-score. Comparative analysis with advanced models confirms the efficiency and robustness of the suggested approach. The model also shows minimal overfitting and high consistency, making it suitable for clinical application. Overall, AMFO-FNN offers a highly accurate and computationally efficient solution for automated brain tumor diagnosis*.

Keywords: *Brain tumor image classification, AMFO-FNN, gaussian filter, GLCM, medical imaging*.

Received February 11, 2025; accepted July 28, 2025
https://doi.org/10.34028/iajit/22/6/13

1. Introduction

Brain tumors pose bold challenges in the intricate realm of neurological conditions, providing good-sized limitations for both sufferers and scientific practitioners [1]. These bizarre growths, originating within the brain or its adjacent tissues, disrupt the difficult equilibrium of the principal anxious gadget Central Nervous System (CNS), frequently to extreme repercussions [24]. A comprehensive draw close of the biological aspects of mind tumors is critical for specific diagnosis, treatment, and dealing with these complex illnesses. Brain tumors develop as abnormal lumps of tissue that grow in the brain or surrounding areas [9]. These tumors are categorized into two fundamental categories based totally on their supply, primary tumors that originate inside the brain itself and metastatic tumors that rise from malignant cells spreading from other parts of the frame [11]. The actual causes in the back of the improvement of mind tumors stay uncertain, even though numerous dangerous elements were identified. These elements include genetic predisposition, exposure to ionizing radiation, certain hereditary conditions, and immune machine disorders. While some chance elements can be mitigated through lifestyle modifications, others like genetic susceptibility gift inherent challenges in the phase of prevention [14].

When a brain tumor appears, various symptoms might crop up. The size, position, and growth rate of the tumor heavily influence these symptoms. Usual signs include persistent headaches, seizure-s, mental issues, shifts in personality or behavior, weakness or begotte-n paralysis, and troubles with vision [25]. However, it's not easy to identify these symptoms specifically in brain tumors. They often mirror signs of other brain-related illnesses, confusing diagnoses. Doctors use a mixture of exams to categorize and pinpoint the tumor. Neurological evaluations, imaging scans like Magnetic Resonance Imagin (MRI) or Computed Axial Tomography (CT), and occasionally, biopsy are used to confirm the tumor type [17]. The healing path a patient follows depends on multiple aspects. Therapies could include surgery, radiation, chemo, specially targeted medicine, and immunotherapy [4]. Is this therapy aimed at eliminating the tumor reducing symptoms and preventing recurrence but minimizing damage to normal brain tissue? A multidisciplinary approach including neurosurgeons oncologists' radiation therapists and other professionals is necessary for selecting a treatment plan through meticulous study [22].

A patient with a brain tumor has a very general range of prognosis because of the tumor type, stage, and response to treatment [12]. Procedures such as surgery to remove benign tumor types normally have a good prognosis and usually result in a speedy recovery,

however, malignant tumors pose more challenges and have poor results. The introduction of new technologies and patient management approaches in healthcare contributes to an increase in the probability of recovery and the quality of survival for a lot of people with brain tumors and brings hope even for those with the profound diagnosis [24].

This research paper is aimed at enhancing the brain tumor image classification precision by using the proposed Adaptive Moth Flame Optimized Feedforward Neural Networks (AMFO-FNN) technique. This goal is accomplished by the relation of Moth Flame Optimized (MFO) and Feedforward Neural Network (FNN) which comprise the features of two different optimization approaches and Neural Networks (NNs).

1.1. Contribution of the Research

1. Brain tumor images sourced from Kaggle provide a valuable dataset for research in medical imaging, enabling the development.
2. The collected images were pre-processed through the filter employed with the Gaussian filter, which decreases noise and increases the quality of the images before analysis.
3. Features are extracted by measuring the spatial correlations between pixel intensities in an image using the Gray-Level Co-occurrence Matrix (GLCM), providing textural information for image analysis and classification applications.
4. A novel method of AMFO-FNN utilized for classification of brain tumor images.

2. Literature Review

The Mutual Information-Accelerated Singular Value Decomposition (MI-ASVD) approach was examined for brain image classification [3]. MI-ASVD exceeded Principal Component Analysis (PCA) and Singular Value Decomposition (SVD) in terms of accuracy. However, more validation on varied datasets and research on computing efficiency was required.

A highly accurate diagnostic model was created for identifying brain cancers in MRI images while reducing the dangers associated with invasive biopsy procedures [5]. The suggested model has superior accuracy, making it a viable non-invasive approach for clinical tumor identification.

Hyperspectral imaging was used to investigate tumor location in the brain [20]. To discover ideal values, it utilized k-based clustering combined with the firefly method. Multilayer FNN marks brain areas. The quality and accessibility of hyperspectral image data were critical to the suggested technique's efficacy.

An effective brain tumor detection technique was evaluated, which employed hybrid classification with MRI data [23]. The approach includes identification with a Neural Network-Convolutional Neural Network (NN-CNN) hybrid classifier optimized via Crossover Operated Rooster-based Chicken Swarm Optimization (COR-CSO) which was developed for accurate brain tumor identification, hence improving diagnostic abilities for medical imaging.

The accuracy of brain tumor identification was improved using CNN [19]. It described a revolutionary method that combines image-enhancing techniques. Despite its effectiveness, drawbacks include image quality fluctuations and the requirement for further validation across many datasets.

A brain tumor classification method was created that combines Deep Learning (DL) application with traditional Machine Learning (ML) classifiers [21]. They succeeded in identifying brain tumors with great accuracy by classifiers. Constraints, such as data set dependency and the need for the experiment to be tested on various datasets, were encountered.

A modern machine was presented for the early and precise detection of mind tumors, which turned into an incredibly critical task [18]. The approach made use of a redesigned CNN for detecting tumor location. There was also the need for further authentication in clinical settings.

A unique Artificial Intelligence (AI) strategy for brain tumor classification that combines the hybrid extraction of features and a Regularized Extreme Learning Machine (RELM) [6]. The method was tested on a newly available open dataset and showed effective classification performance. However, the study lacked detailed validation and generalizability across diverse datasets.

A breast tissue cancer identification strategy was provided to extract a procedure to differentiate between normal and malignant breast tissues [8]. The used features were loaded into an FNN classifier that was observed to provide far better classification accuracy than previous studies.

A new type of framework was developed for the recognition and classification of cancer tumors in MRI images [2]. It used Particle Swarm Optimization (PSO) for segmentation and Convolutional Neural Networks (CNNs) for classification. Precise performance was demonstrated particularly in comparison to the traditional ones.

The limitations of Artificial Neural Networks (ANN) in medical image classification were addressed, particularly in detecting abnormalities in brain MR images [7]. They were expected to provide faster convergence and higher accuracy under the same iteration conditions as the conventional Counter-Propagation Network (CPN) and Kohonen networks. Experimental findings have shown that brain images with aberrancies can be effectively classified.

A machine vision-based brain tumor classification model was created utilizing MRI data to solve the delayed and inefficient diagnostic procedure [15, 16]. A unique hybrid framework was developed and tested for categorizing various forms of brain tumors. However,

constraints might exist, such as the necessity for additional validation and testing in a broad sample.

2.1. Research Gap

While recent algorithms have improved brain tumor classification, fundamental limitations remain. CNNs and COR-CSO are highly accurate but computationally demanding and not interpretable for clinical purposes [19]. Single-dataset AlexNet-based approaches tend to be non-generalizable [18]. Hyperspectral imaging is severely data-dependent, diminishing robustness [20]. Numerous studies lack vital statistical protocols such as k-fold cross-validation and standard deviation reporting, impacting reproducibility [8]. Feature selection methods like MI-ASVD have no rationale for chosen features [3], and wavelet-based approaches don't explicitly report their dimensionality reduction methodologies [2]. Harris Hawks Optimized Convolution Network (HHOCNN) models also depend on manually designed features with high training costs [23]. In contrast, the introduced AMFO-FNN incorporates GLCM-based features and AMFO to design a lightweight, interpretable, and statistically robust model. It has cross-validation, reports standard deviation, and works well on the Br35H dataset, showing better accuracy, efficiency, and clinical relevance than standard and Deep Learning (DL) approaches.

3. Methodology

In the methodology section, AMFO-FNN for brain tumor image classification. The data set was collected from Kaggle. Pre-processing using Gaussian filter. Then, the feature extraction utilized GLCM. Figure 1 demonstrates the methodology flow.

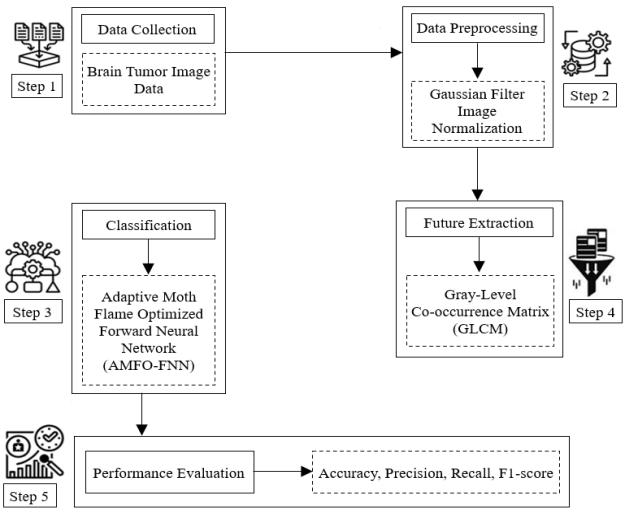

Figure 1. Methodology flow of the AMFO-FNN method.

3.1. Dataset

The brain tumor image data employed was the open source Br35H dataset, acquired from Kaggle [27]. The dataset is comprised of 7,023 T1-weighted contrast-enhanced MRI images belonging to four classes: glioma, meningioma, pituitary tumor, and no tumor. The images are all unique patient cases and have different sizes and resolutions. To ensure consistency in model input, all the images were resized to 256×256 pixels. The "no tumor" category contains images that show no sign of abnormal growth and are an important negative control for the classification task. To provide a strong and unbiased model evaluation, the data was split with a stratified 80:20 train-test split to have balanced class distributions within both sets. Additionally, the research utilized 5-fold cross-validation on the train data to determine the model's generalizability. All the reported performance metrics are the average five-fold, and the standard deviation is used to indicate variability and reliability across runs.

The Br35H dataset consists of a total of 7,023 images that are distributed across four classes: glioma (1,426 images), meningioma (1,448 images), pituitary tumor (1,413 images), and no tumor (2,736 images). The distribution is not extremely unbalanced, with the "no tumor" class having significantly more samples. To counter any bias at training time, stratified sampling was performed at dataset splitting and data augmentation was used for underrepresented classes.

3.2. Gaussian Filter for Data Pre-Processing

Data pre-processing with a Gaussian filter for brain tumor image classification involves performing a Gaussian smoothing operation on the image. This filter reduces noise and enhances essential image elements, making them better suited for analysis and classification applications. The Gaussian filter is used for more efficient image flattening. It is the initial stage of detection of noise; however, it is not particularly efficient at eliminating pepper and salt sounds. It is derived from the Gaussian distribution.

The probability concentration function in Equation (1) represents the probability density function of a Gaussian distribution, denoted as $O(w)$.

$$O(w) = \frac{1}{\sqrt{2\pi\sigma^2}} f^{-(w-\mu)^2/(2\sigma)^2} \quad (1)$$

w represents a grayscale image, μ denotes the mean value and σ stands for the standard deviation.

The Gaussian's standard deviation (σ) controls the level of flattening.

Besides noise attenuation by applying a Gaussian filter, image normalization was also done to normalize pixel intensity values between [0, 1] for faster convergence and training stability. For balancing class and increasing the diversity of the dataset, data augmentation techniques of random rotations (±15°), horizontal and vertical flips, and zoom (90-110%) were applied. The augmentations were applied only to the training dataset and avoided overfitting and increased the model's generalization.

3.3. Gray-Level Co-Occurrence Matrix (GLCM) for Feature Extraction

Extracting features in classification of brain tumor image using GLCM. This algorithm leverages GLCM for characterizing the association between local pixel intensities in medical images, thereby allowing for the recognition of distinctive patterns indicative of brain tumors. The GLCM, a feature extraction tool, was used for this study. Firstly, the picture was altered to be in black and white. Then, the window size to draw the correlation between the brightness of the central pixel and the brightness of its surroundings. This link between elements was formulated as a matrix, which identifies the frequency that the pixels renew their suspected direction consecutive. By using the correlation between the pixel intensities, GLCM gave shape to the texture derived from the grayscale, to the kernel applied, and to the direction. The study investigated the fourteen textural features but only chose six particular features relevant to this research to significantly reduce the spatial context information, which is an overhead that can be a disadvantage factor in the classification process. Texture analysis takes a look at the contrast and uniformity of images; it also measures the similarity of different parts of the same image and then computes by means of the evaluation of the following indicators: the Angular Second Moment (ASM), energy, and correlation. Even though GLCM gives 14 default texture features, we chose six features contrast, energy, homogeneity, entropy, correlation, and dissimilarity according to a feature ranking experiment on mutual information and classification effect. The six features gave the optimal tradeoff between classification accuracy and computational complexity with noise reduction of irrelevant features.

- **Correlation**: the distance between an image's brightest areas to its darkest, which is known as the ridge line, is computed within the luminance of the pixels. This is information about how bright a good pixel is compared to the intensity of its neighbors, Equation (2).

$$Correlation = \sum_{i=0}^{N-1}\sum_{i=0}^{N-1}\frac{(i-\mu_i)(j-\mu_j)}{\sqrt{(\sigma_i)(\sigma_j)}} \quad (2)$$

- **Contrast**: contrast is the difference in intensity between close pixels. Higher contrast indicates more variability in intensity values, Equation (3).

$$Contrast = \sum_{i=0}^{N-1}\sum_{i=0}^{N-1}(i-j)^2 \quad (3)$$

- **Uniformity**: often referred to as the reverse distinction moment, this measurement evaluates the uniformity or evenness of an image. Elevated values of uniformity imply a lesser deviation in brightness amongst adjacent pixels, Equation (4).

$$Uniformity = \sum_{i=0}^{N-1}\sum_{i=0}^{N-1}\frac{p(i,j)}{1+(i-j)^2} \quad (4)$$

- **Energy**: energy refers to the square root of a picture's second-moment angle, gauging the overall spread of its brightness. A high energy value suggests a texture that is well arranged or uniform in its distribution, Equation (5).

$$Energy = \sqrt{\sum_{i=0}^{N-1}\sum_{i=0}^{N-1}p(i,j)^2} \quad (5)$$

- **Dissimilarity**: calculating the difference between the mean high and low in pixels in a particular area. Bigger scattering ratings would mean more variation in brightness values, Equation (6).

$$Dissimilarity = \sum_{i=0}^{N-1}\sum_{i=0}^{N-1}p(i,j)x|i-j| \quad (6)$$

- **ASM**: establishes functions that determine whether given pixel pairs are homogeneous or not. It counts the distinct frequencies of gray pairings and displays high values in images that have a similar texture, Equation (7).

$$Angular\ Second\ Moment = \sum_{i=0}^{N-1}\sum_{i=0}^{N-1}p(i,j)^2 \quad (7)$$

The pursuit of crafting textural features, we employed grayscale images of the dimensions 100x100 and a kernel that is 19 units in size. This approach threw up 48 distinct features for each image, each having a spacing of either 1 or 2 and a specific rotation pegged at 0°, 45°, 90°, or 135°. Every feature receives normalization to sum up to one and N stands as a numerical representation of the gray levels.

3.4. Classification Using Adaptive Moth Flame Optimized Feedforward Neural Networks (AMFO-FNN)

AMFO-FNN employs a particular supervised learning method when it comes to classifying glioma images. It employs a modulated moth flame optimization technique and FNNs that boost the classification accuracy. This strategy with weights and biasing parameters leads to better network suitability to categorize brain tumor images, thus being more used in medical diagnosis and treatment plans.

3.4.1. Adaptive Moth Flame Optimization (AMFO)

The MFO algorithm was changed by the addition of the Levy flight and the Cauchy operators. Herein, the standard MFO Equation (10) portrays its efficiency in arriving at the optimal solution given enough computation time. Yet, it cannot avert a relatively slow search. In order to retain the searching ability of MFO without the loss of exploration features, enhanced search operations such as those available in the adaptive

Cuckoo search algorithm are proposed to be utilized. A flowchart of an adaptive approach to MFO is shown in Figure 2.

$$S(M_i, F_j) = D_j e^{bt} \cos(2\pi t) + F_j \quad (8)$$

In the conventional MFO algorithm, the moth moves based on the distance from the moth to the flame. In the new update, we would like to incorporate the step size which will depend on the best, worst, and current moth position. The step size will manage the distance from the current position to the new position of the moth. Equation (9) indicates that, because the number of iterations will increase, the generation turns inversely proportional to the step size, where the step size decreases. Further, Equation (10) uses the computed step size to advance the moth to another position.

$$X_i^{t+1} = \left(\frac{1}{t}\right)^{\left|\frac{(best\ f(t) - f_i(t))}{best() - worstf}\right|} \quad (9)$$

$$Moth_{post(t+1)} = Moth_{pos(t)} + p * X_i^{t+1} \quad (10)$$

Equation (21) provides a degree of arbitrariness in the position update equation. The next part presents the performance results and comparative analysis of the proposed AMFO using a set of conventional single-objective benchmark functions with varying features. Figure 2 and Table 1 represents the flow of the AMFO model.

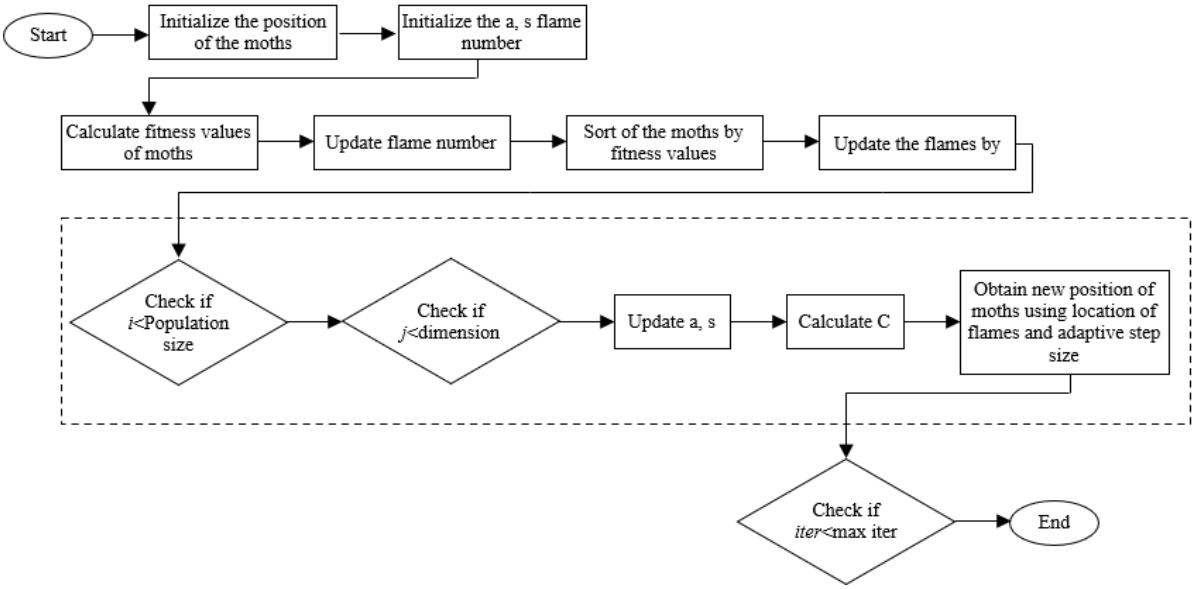

Figure 2. Flow of the AMFO model.

Table 1. Hyperparameter table for AMFO-FNN.

Hyperparameter	Symbol/Name	Typical value(s)	Description
Number of moths	N	10-100	Size of the population (number of candidate FNN solutions).
Number of flames	F	Equal to N	Top-performing moths used to guide optimization.
Maximum iterations	$T_{\{max\}}$	50-500	Total number of optimization iterations.
Dimensionality	D	Depends on the FNN structure	Number of parameters (weights + biases) to optimize.
Adaptive spiral coefficient	a	-1 to -2 (linearly decreasing)	Controls the contraction rate of the spiral function.
Spiral shape constant	b	1	Affects the tightness of the logarithmic spiral path.
Randomization factor	t	Uniform [a, 1]	Random value controlling the angle in the spiral update.
Mutation rate (adaptive)	μ	0.01-0.1	Probability of random mutation for diversity (used adaptively).
Learning rate (optional)	η	0.001-0.01	Used if adaptive learning or hybrid training is incorporated.
Activation function	-	Sigmoid, ReLU, Tanh	Activation is used in the FNN hidden/output layers.
Loss function	-	MSE, CE	Measures prediction error during fitness evaluation.
Dataset split ratio	-	80% training/20% testing	Proportion of data used to evaluate each candidate FNN.
Network topology	-	Input-hidden-output (e.g., 3-4-1)	Defines the architecture of the FNN.

3.4.2. Feedforward Neural Network

Let's simplify the essential idea of an ANN. Basically, an ANN has layers with various connected parts. They work on the data that feeds them to give results. To make it easy:

- Input and output: the ANN starts with a data input (x) and in the end, produces an output (y), representing a category-based variable.
- Layers: the ANN has several layers (l). Each layer has certain units (m). All layers, except the last one, are hidden. The last one is the output layer.
- Weights and biases: each link between different layers holds a weight w_{ij}^k. This weight shows how strong the connection is. Plus, each layer has its own bias $b^{l+1} \in \mathbb{R}$).
- Activation functions: these are the rules $s_i^k(.))$ that decide the output of each unit. They use both the weights and biases. Common choices are the logistic sigmoid and hyperbolic tangent functions.
- Processing flow: input data gets a weight and then goes through activation functions in each layer. Each

layer then makes outputs which become inputs for the next layer. This cycle happens over and over until the output layer gives the final result.

Data entry into the entanglement is the first layer and is the first step towards calculating entanglement weights. Equation (11) which is the input data, is used to reckon the activations of the units in the first layer.

$$h_i^1 = s_i^{k+1}\left(b^1 + \sum_{j=1}^{m} w_{ij}^{k+1}\, x_j\right) \tag{11}$$

We next estimate the activation functions $s_i^i(.)$ for the second layer after getting the outputs of the first layer. Equation (12) is used to compute the activations of the units in the subsequent layer based on the activations of the units in the previous layer.

$$h_i^{k+1} = s_i^{k+1}\left(b^{k+1} + \sum_{j=1}^{m} w_{ij}^{k+1}\, h_i^k\right) \tag{12}$$

The estimated probability of the output is calculated after passing through each hidden layer k sequentially to the final output, Equation (13).

$$\hat{y} = b^{l+1} + \sum_{j=1}^{m} w_{ij}^{k+1}\, h_i^k \tag{13}$$

In the estimating procedure mentioned previously, the activation functions (.) is essential. In our investigation, we employ the logistic function, which is commonly utilized as a nonlinear activation function, Equation (14).

$$s(x) = \frac{1}{1 + \exp(-x)} \tag{14}$$

This estimation is, however, a procedure, which can be regarded as the adaptation of the weights of the network by iterative learning in response to data. A neural network adapts the weights (w_{ij}^k) one after the other, for each layer (k) and each neuron (i) in it. The performance of the network is gauged on those weights discovered during the training period. The next stage is to apply a cost function to achieve the approximation to the value of weights in the network. The cost function, which serves as the learning goal function should be minimized. The Mean Square Error (MSE), or Equation (15), is the most widely used value function.

$$E = \frac{1}{N}\sum_{i=1}^{N} (y_i - \hat{y}_1)^2, \tag{15}$$

Cross-Entropy (CE), a popular cost function, considers both category variables and input data vectors.

$$S = -\sum_{i=1}^{N} p_i \log q_i \tag{16}$$

Here, according to Equation (16), p_i and q_i are continuous possibilities.

Network weight estimate frequently suffers from overfitting, which impairs the generalization of new data. This happens when the network gives training data performance a higher priority than test data performance. A possible way of reducing overfitting is through regularization during estimation by adding a term proportional to the sum of the square weights in the cost function to punish it and that improves network generalization performance. Characteristically, this regularization process can be described using the MSE cost function in the general form as, Equation (17).

$$E_{reg} = \gamma \sum_{k=i}^{l} \sum_{i,l=1}^{m} \left(w_{ij}^k\right)^2 + (1-\gamma)E = \gamma E_w + (1-\gamma)E, \tag{17}$$

$\gamma \in (0,1)$ is the regularization constant. To optimize estimate procedures and ensure convergence, Equation (16) is commonly improved by the gradient descent technique and the backpropagation method. AMFO-FNN detects patterns and appropriately solves an optimization problem, it will depict a rigid and flexible way to handle hard problems, as depicted in the AMFO-FNN Algorithm (1).

Algorithm 1: Process of AMFO-FNN.

```
Initialize parameters
initialize_network()
Define moth flame optimization parameters
initialize_AMFO_parameters()
Training process
for epoch in range(num_epochs):
  Forward propagation
   for each training_example in training_data:
      output = forward_propagation(training_example)
      Calculate loss
      loss = calculate_loss(output, expected_output)
  Backward propagation
backward_propagation(loss)
  Update network parameters using AMFO
moth_flame_optimization()
  Print progress
   if epoch % print_interval == 0:
print("Epoch:", epoch, "Loss:", total_loss)
Prediction process
for example in test_data:
   prediction = forward_propagation(example)
print("Prediction:", prediction)
```

4. Performance of Evaluation

All calculations were performed employing an Intel Core i7-7800 3.5 GHz CPU. An NVIDIA GeForce GTX 1080 Ti GPU can be utilized for smart modification and version training. Python 3.7 is operational and it processes, evaluates, and visualizes records. The platform was delighted to have adequate RAM capacity (32 GB), allowing it to run and work gently with scientific research material.

4.1. Performance Comparison

A comparative performance comparison of different brain tumor classification techniques tested over a

benchmarked MRI dataset. The suggested AMFO-FNN model is compared with the latest methods, such as HHOCNN [10], AlexNet with Extreme Learning Machine (ELM) [27], and Batch Normalized AlexNet-ELM optimized by Chaotic Bat Algorithm (BN-AlexNet-ELM-CBA) [13]. The classification performance of each model is evaluated by accuracy, precision, recall, and F1-score. The comparison of performances of different brain tumor classification models illustrates that the suggested AMFO-FNN model performs better than any other approach on major evaluation measures. A particular maximum accuracy of 99.14% shows how well the model can classify both tumor and non-tumor cases. The model also achieves a precision of 98.95%, representing high reliability in making accurate tumor case identification among all positive predictions. The model's recall (99.21%) indicates its remarkable ability to identify true tumor cases, and it is extremely important in medical diagnosis to reduce missed detections. Additionally, the F1-score of 99.08% indicates a highly balanced performance between precision and recall, which further assures the robustness and clinical importance of the model. Furthermore, compared with the HHOCNN model, whose performance was slightly lower but still competitive, the AlexNet+ELM and BN-AlexNet-ELM-CBA models achieved relatively moderate performance. Generally, AMFO-FNN provides the most precise, consistent, and reliable results among the tested methods and hence remains the best method for detecting brain tumors.

Table 2 and Figures 3, 4, and 5 represent the output of the comparison of key metrics.

Table 2. Comparative performance of brain tumor classification models using MRI images.

Methods	Accuracy (%)	Precision (%)	Recall (%)	F1-score (%)
HHOCNN [10]	98.00	97.90	98.70	98.80
AlexNet + ELM [27]	96.00	94.00	94.00	96.00
BN-AlexNet-ELM-CBA [13]	96.43	96.17	97.14	96.50
AMFO-FNN [Proposed]	99.14	98.95	99.21	99.08

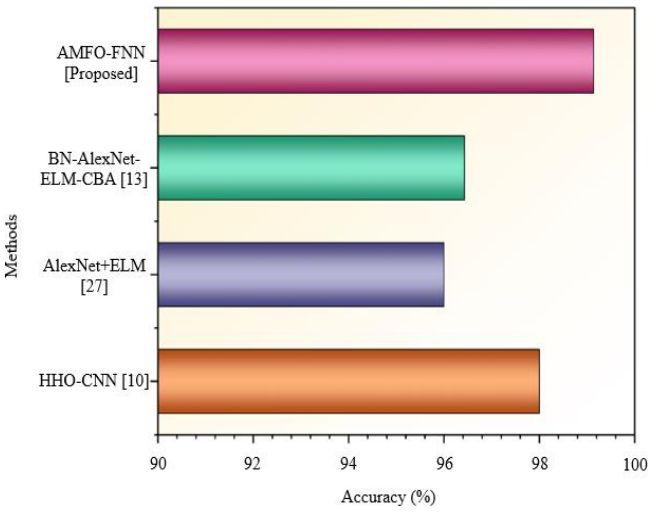

Figure 3. Comparative accuracy analysis of brain tumor detection techniques.

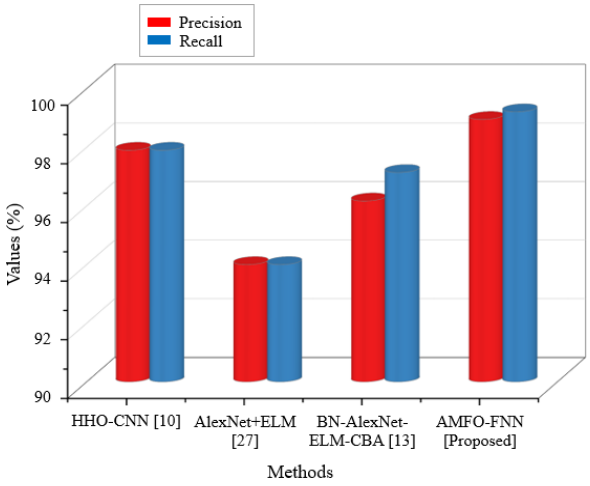

Figure 4. Evaluation of precision and recall rates across different classification models.

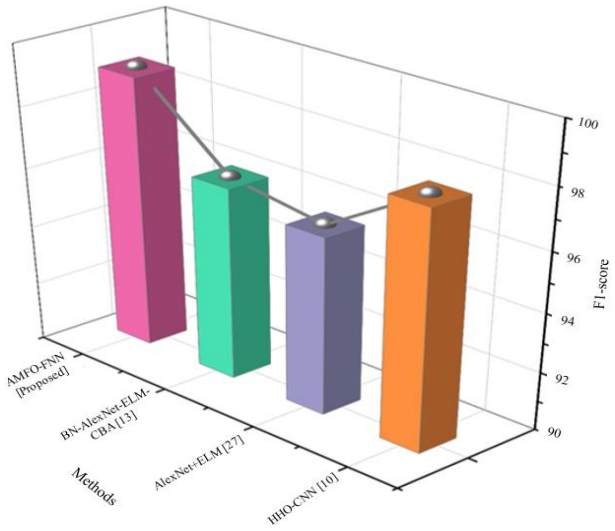

Figure 5. F1-score performance comparison for brain tumor classification approaches.

Table 3 shows the five-fold cross-validation results of the AMFO-FNN model, confirming its stable performance.

Table 3. Five-fold cross-validation results of the AMFO-FNN model.

Fold	Accuracy (%)	Precision (%)	Recall (%)	F1-score (%)
Fold 1	98.95	98.70	99.10	98.85
Fold 2	99.30	99.10	99.40	99.25
Fold 3	99.00	98.80	99.20	99.00
Fold 4	99.40	99.20	99.30	99.20
Fold 5	99.10	99.00	99.05	99.10
Mean±SD	99.14±0.17	98.95±0.18	99.21±0.13	99.08±0.14

4.2. Confusion Matrix

The training accuracy rises steadily to over 90%, while the validation accuracy plateaus at over 82%, indicating good learning and generalization. Meanwhile, the training loss decreases step by step, and the validation loss demonstrates declining behavior with very little overfitting. The shallow disparity in the training and validation curves specifies that the model performs well with high performance and without extreme variance between observed and unobserved data. Figure 6 provides the training and validation accuracy and loss

curves for 10 epochs.

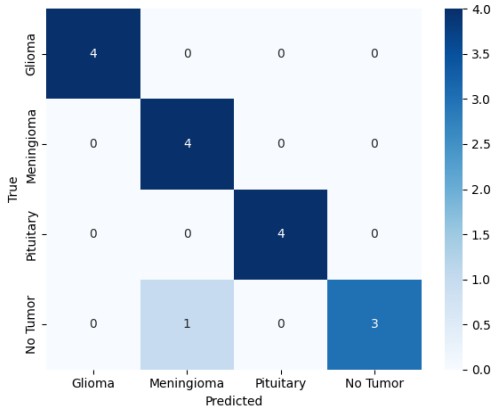

Figure 6. Confusion matrix of AMFO-FNN.

4.3. Accuracy and Loss

The matrix shows high classification accuracy of all four classes: glioma, meningioma, pituitary, and no tumor. Ideal classification for the first three classes of tumors and one misclassification among the "no tumor" class were achieved, where the sample was wrongly classified as meningioma. The matrix shows the efficiency and effectivity of the proposed method in multi-class brain tumor image classification. The impressive ability of the model to classify in a diagonal-dominant fashion can be seen in the matrix. It is only between no tumor and meningioma that it gets confused, and it indicates slight feature representation overlap for these classes. Figure 7 shows the confusion matrix for the AMFO-FNN model on the test set.

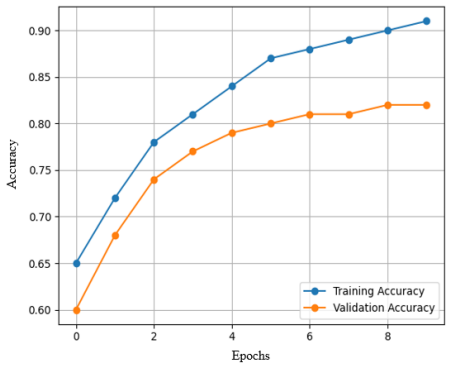

a) Training and validation accuracy.

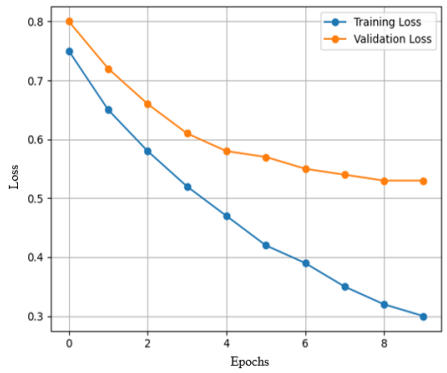

b) Training and validation loss.

Figure 7. Training and validation accuracy/loss curves across epochs.

4.4. ROC Curve Analysis

The ability to differentiate tumor vs. non-tumor cases from MRI images. The Receiver Operating Characteristic (ROC) curve graphically shows the True Positive Rate (TPR) against the False Positive Rate (FPR) over various classification thresholds. Area Under the Curve (AUC) value obtained with 0.9497, shows an extremely high discriminative power of the model. An AUC of near 1.0 indicates that the model has a good ability to differentiate between tumor and non-tumor samples with very few misclassifications or errors. The sharp upturn in the top-left corner shows that the model can attain a very high TPR at low FPRs. This outcome confirms the strength and clinical value of the AMFO-FNN model in effectively classifying brain tumors. Figure 8 shows the ROC curve of the proposed AMFO-FNN model.

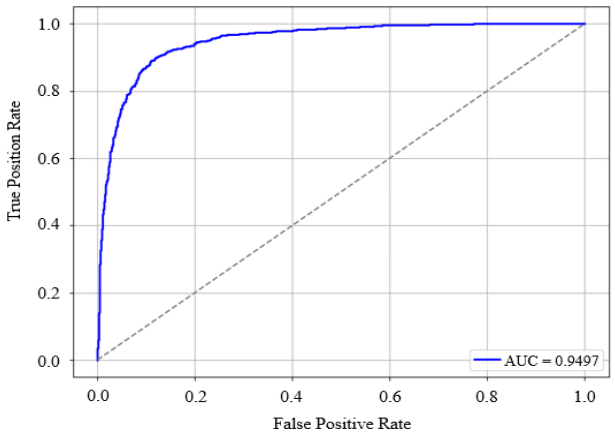

Figure 8. ROC curve with AUC for the AMFO-FNN model.

4.5. Discussion

The performance comparison of the proposed AMFO-FNN model and other brain tumor classification models shows that the proposed model evidently outperforms other classification models. It has the best value in all evaluation criteria among all tested models. HHOCNN [10], AlexNet+ELM [27], and BN-AlexNet-ELM-CBA [13] have comparatively lower performance in all criteria. Additionally, unsupervised autoencoder-based multimodal fusion methods [26] face limitations such as the need for larger datasets to improve generalization and the absence of validation in real-time clinical hardware. The high performance of AMFO-FNN also reveals its efficiency in precisely classifying tumor cases with a very good sensitivity-specificity balance. Its capacity for optimizing feature learning and classification makes it an effective and stable method for the diagnosis of brain tumors from MRI images. A comparative experiment was conducted to examine the impact of preprocessing steps. Models without Gaussian filtering and normalization suffered a 4-6% decline in accuracy and a greater variance in cross-validation results, supporting the effectiveness of our preprocessing pipeline in stabilizing learning and

improving classification performance. Training and validation loss curves for the model were tracked to check for overfitting. They demonstrated good convergence with minimal divergence, showing that the model generalizes well for new data. Dropout and early stopping were employed during training to prevent overfitting further.

5. Conclusions

Brain tumor classification utilizing medical imaging entails assessing images like MRI scans to classify tumors based on their features, assisting in diagnosis as well as planning for treatment. The study introduced AMFO-FNN for brain tumor image classification. By combining the advantages of MFO and FNN, the proposed method significantly improves classification accuracy over previous methods. The data was collected from Kaggle. Pre-processing used a Gaussian filter. GLCM for feature extraction helped refine the input data for classification. Evaluation factors including 99.21% recall, 98.95% precision, 99.08% F1-score, and 99.14% accuracy revealed that the AMFO-FNN method outperformed state-of-the-art methods. These findings on brain tumors demonstrate the potential of the proposed method to improve early detection and treatment planning, leading to better patient outcomes. The proposed method efficiently classifies brain tumor images, and could assist physicians make more educated decisions, ultimately improving the overall treatment of brain tumor patients.

5.1. Limitation and Future Scope

The availability and quality of labeled data are one of the most significant obstacles in developing effective algorithms for brain tumor classification. High-quality labeled datasets are critical for training strong models, but collecting them might be difficult due to privacy issues and restricted access to medical images along with the differences in image-capturing methodologies. Combining data collected through various imaging modalities, including MRI, CT and Positron Emission Tomography (PET) scans, can lead to an improved comprehension of brain tumors. Future research might focus on creating models that can successfully combine data from several imagined sources to increase classification accuracy.

Data Availability

https://www.kaggle.com/datasets/masoudnickparvar/brain-tumor-mri-dataset

References

[1] Abd-Ellah M., Awad A., Khalaf A., and Hamed H., "A Review on Brain Tumor Diagnosis from MRI Images: Practical Implications, Key Achievements, and Lessons Learned," *Magnetic Resonance Imaging*, vol. 61, pp. 300-318, 2019. https://doi.org/10.1016/j.mri.2019.05.028

[2] Ali M., Shah J., Khan M., Alhaisoni M., and et al., "Brain Tumor Detection and Classification Using PSO and Convolutional Neural Network," *Computers, Materials and Continua*, vol. 73, no. 3, pp. 4501-4518, 2022. https://doi.org/10.32604/cmc.2022.030392

[3] Al-Saffar Z. and Yildirim T., "A Novel Approach to Improving Brain Image Classification Using Mutual Information-Accelerated Singular Value Decomposition," *IEEE Access*, vol. 8, pp. 52575-52587, 2020. https://doi.org/10.1109/ACCESS.2020.2980728

[4] Anand U., Dey A., Chandel A., Sanyal R., and et al., "Cancer Chemotherapy and Beyond: Current Status, Drug Candidates, Associated Risks and Progress in Targeted Therapeutics," *Genes and Diseases*, vol. 10, no. 4, pp. 1367-1401, 2023. https://doi.org/10.1016/j.gendis.2022.02.007

[5] Basaran E., "A New Brain Tumor Diagnostic Model: Selection of Textural Feature Extraction Algorithms and Convolution Neural Network Features with Optimization Algorithms," *Computers in Biology and Medicine*, vol. 148, pp. 105857, 2022. https://doi.org/10.1016/j.compbiomed.2022.105857

[6] Gumaei A., Hassan M., Hassan M., Alelaiwi A., and Fortino G., "A Hybrid Feature Extraction Method with Regularized Extreme Learning Machine for Brain Tumor Classification," *IEEE Access*, vol. 7, pp. 36266-36273, 2019. https://doi.org/10.1109/ACCESS.2019.2904145

[7] Hemanth D., Vijila C., Selvakumar A., and Anitha J., "Performance Improved Iteration-Free Artificial Neural Networks for Abnormal Magnetic Resonance Brain Image Classification," *Neurocomputing*, vol. 130, pp. 98-107, 2014. https://doi.org/10.1016/j.neucom.2011.12.066

[8] Kavitha A. and Chellamuthu C., "Brain Tumor Detection Using Self-Adaptive Learning PSO-based Feature Selection Algorithm in MRI Images," *International Journal of Business Intelligence and Data Mining*, vol. 15, no. 1, pp. 71-97, 2019. https://doi.org/10.1504/IJBIDM.2019.100469

[9] Khan F., Gulzar Y., Ayoub S., Majid M., and et al., "Least Square-Support Vector Machine Based Brain Tumor Classification System with Multi Model Texture Features," *Frontiers in Applied Mathematics and Statistics*, vol. 9, pp. 1-17, 2023. https://doi.org/10.3389/fams.2023.1324054

[10] Kurdi S., Ali M., Jaber M., Saba T., and et al., "Brain Tumor Classification Using Meta-Heuristic Optimized Convolutional Neural Networks," *Journal of Personalized Medicine*,

vol. 13, no. 2, pp. 1-18, 2023. https://doi.org/10.3390/jpm13020181

[11] Lah T., Novak M., and Breznik B., "Brain Malignancies: Glioblastoma and Brain Metastases," *Seminars in Cancer Biology*, vol. 60, pp. 262-273, 2020. https://doi.org/10.1016/j.semcancer.2019.10.010

[12] Le Rhun E., Guckenberger M., Smits M., Weller M., and Preusser M., "EANO-ESMO Clinical Practice Guidelines for Diagnosis, Treatment and Follow-up of Patients with Brain Metastasis from Solid Tumors," *Annals of Oncology*, vol. 32, no. 11, pp. 1332-1347, 2021. https://doi.org/10.1016/j.annonc.2021.07.016

[13] Lu S., Wang S., and Zhang Y., "Detection of Abnormal Brain in MRI via Improved AlexNet and ELM Optimized by Chaotic Bat Algorithm," *Neural Computing and Applications*, vol. 33, no. 17, pp. 10799-10811, 2021. https://doi.org/10.1007/s00521-020-05082-4

[14] Lumniczky K., Impens N., Armengol G., Candeias S., and et al., "Low dose Ionizing Radiation Effects on the Immune System," *Environment International*, vol. 149, pp. 106212, 2021. https://doi.org/10.1016/j.envint.2020.106212

[15] Nawaz S., Khan D., and Qadri S., "Brain Tumor Classification Based on Hybrid Optimized Multi-Features Analysis Using Magnetic Resonance Imaging Dataset," *Applied Artificial Intelligence*, vol. 36, no. 1, pp. 1951-1977, 2022. https://doi.org/10.1080/08839514.2022.2031824

[16] Nickparvar M., Kaggle, Brain Tumor MRI Dataset, https://www.kaggle.com/datasets/masoudnickparvar/brain-tumor-mri-dataset, Last Visited, 2025.

[17] Overcast W., Davis K., Ho C, Hutchins G., and et al., "Advanced Imaging Techniques for Neuro-Oncologic Tumor Diagnosis, with an Emphasis on PET-MRI Imaging of Malignant Brain Tumors," *Current Oncology Reports*, vol. 23, pp. 1-15, 2021. https://doi.org/10.1007/s11912-021-01020-2

[18] Ramtekkar P., Pandey A., and Pawar M., "Innovative Brain Tumor Detection Using Optimized Deep Learning Techniques," *International Journal of System Assurance Engineering and Management*, vol. 14, no. 1, pp. 459-473, 2023. https://doi.org/10.1007/s13198-022-01819-7

[19] Rasheed Z., Ma Y., Inam Ullah., Ghadi Y., and et al., "Brain Tumor Classification from MRI Using Image Enhancement and Convolutional Neural Network Techniques," *Brain Sciences*, vol. 13, no. 9, pp. 1320, 2023. https://doi.org/10.3390/brainsci13091320

[20] Rinesh S., Maheswari K., Arthi B., Sherubha P., and et al., "Investigations on Brain Tumor Classification Using Hybrid Machine Learning Algorithms," *Journal of Healthcare Engineering*, vol. 2022, no. 1, pp. 1-9, 2022. https://doi.org/10.1155/2022/2761847

[21] Sarkar A., Maniruzzaman M., Ashik Alahe M., and Ahmad M., "An Effective and Novel Approach for Brain Tumor Classification Using AlexNet CNN Feature Extractor and Multiple Eminent Machine Learning Classifiers in MRIs," *Journal of Sensors*, vol. 2023, no. 1, pp. 1-19, 2023. https://doi.org/10.1155/2023/1224619

[22] Somma T., Ius T., Certo F., Santi L., and et al., "From the Champion to the Team: New Treatment Paradigms in Contemporary Neurosurgery," *World Neurosurgery*, vol. 131, pp. 141-148, 2019. https://doi.org/10.1016/j.wneu.2019.07.196

[23] Thangarajan S. and Chokkalingam A., "Integration of Optimized Neural Network and Convolutional Neural Network for Automated Brain Tumor Detection," *Sensor Review*, vol. 41, no. 1, pp. 16-34, 2021. https://doi.org/10.1108/SR-02-2020-0039

[24] Thenuwara G., Curtin J., and Tian F., "Advances in Diagnostic Tools and Therapeutic Approaches for Gliomas: A Comprehensive Review," *Sensors*, vol. 23, no. 24, pp. 1-47, 2023. https://doi.org/10.3390/s23249842

[25] Tian Y., Zhou L., Gao J., Jiao B., and et al., "Clinical Features of NOTCH2NLC-Related Neuronal Intranuclear Inclusion Disease," *Journal of Neurology, Neurosurgery and Psychiatry*, vol. 93, no. 12, pp. 1289-1298, 2022. https://doi.org/10.1136/jnnp-2022-329772

[26] Vijayan S. and Subramani M., "Unsupervised Convolutional Autoencoder Framework for Multimodal Medical Image Fusion in Brain Tumour Diagnosis," *The International Arab Journal of Information Technology*, vol. 22, no. 5, pp. 972-985, 2025. https://doi.org/10.34028/iajit/22/5/11

[27] Zhu J., Gu C., Wei L., Li H., and et al., "Brain Tumor Recognition by an Optimized Deep Network Utilizing Amended Grasshopper Optimization," *Heliyon*, vol. 10, no. 7, pp. 1-14, 2024. https://doi.org/10.1016/j.heliyon.2024.e28062

Raafat Munshi is an Assistant Professor in the Department of Medical Laboratory Technology, Faculty of Applied Medical Sciences, King Abdulaziz University, Rabigh, Saudi Arabia. He earned his Ph.D. in Molecular Medicine from Trinity College Dublin, Ireland (2017), his Master's degree in Chemical Analysis and Laboratory Management from the University of New South Wales, Australia (2010), and his Bachelor's degree in Medical Technology from King Abdulaziz University, Saudi Arabia (1999). Before his academic appointment, Dr. Munshi worked (2001-2021) as a Clinical Biochemistry Laboratory Technologist at King Abdulaziz University Hospital. His research interests include Molecular Diagnostics, Cancer Prediction, Artificial Intelligence in Medical Diagnostics, and Clinical Biochemistry. He has published in international peer-reviewed journals such as PLOS ONE, Image and Vision Computing, and Heliyon. Dr. Munshi is also actively engaged in Developing Novel Machine Learning and Ensemble Learning Approaches for disease prediction and has contributed to advancements in COVID-19 diagnosis, Cervical and Breast Cancer Detection, and Proteomic Characterization of Pathogens.